



OPEN ACCESS

Edited by:

Juan Carlos Del Alamo,
University of Washington,
United States

Reviewed by:

Ali Hosseinsabet,
Tehran University of Medical
Sciences, Iran
Lennart Tautz,
Charité—Universitätsmedizin
Berlin, Germany

***Correspondence:**

Mingxing Xie
xiemx@hust.edu.cn
Li Zhang
zli429@hust.edu.cn
Bo Liang
xiehelb@sina.com

†These authors have contributed
equally to this work and share first
authorship

Specialty section:

This article was submitted to
Cardiovascular Imaging,
a section of the journal
Frontiers in Cardiovascular Medicine

Received: 19 June 2021

Accepted: 21 October 2021

Published: 30 November 2021

Citation:

Sun W, Shen X, Wang J, Zhu S,
Zhang Y, Wu C, Xie Y, Yang Y, Dong N,
Wang G, Li Y, Lv Q, Liang B, Zhang L
and Xie M (2021) Association Between
2D- and 3D-Speckle-Tracking
Longitudinal Strain and Cardiovascular
Magnetic Resonance Evidence of
Diffuse Myocardial Fibrosis in Heart
Transplant Recipients.
Front. Cardiovasc. Med. 8:727745.
doi: 10.3389/fcvm.2021.727745

Association Between 2D- and 3D-Speckle-Tracking Longitudinal Strain and Cardiovascular Magnetic Resonance Evidence of Diffuse Myocardial Fibrosis in Heart Transplant Recipients

Wei Sun^{1,2,3†}, Xuehua Shen^{4,5†}, Jing Wang^{4†}, Shuangshuang Zhu^{1,2,3}, Yanting Zhang^{1,2,3}, Chun Wu^{1,2,3}, Yuji Xie^{1,2,3}, Yun Yang^{1,2,3}, Nianguo Dong⁶, Guohua Wang⁶, Yuman Li^{1,2,3}, Qing Lv^{1,2,3}, Bo Liang^{4*}, Li Zhang^{1,2,3*} and Mingxing Xie^{1,2,3*}

¹ Department of Ultrasound, Union Hospital, Tongji Medical College, Huazhong University of Science and Technology, Wuhan, China, ² Hubei Province Clinical Research Center for Medical Imaging, Wuhan, China, ³ Hubei Province Key Laboratory of Molecular Imaging, Wuhan, China, ⁴ Department of Radiology, Union Hospital, Tongji Medical College, Huazhong University of Science and Technology, Wuhan, China, ⁵ Department of Radiology, The Affiliated Hospital of Guizhou Medical University, Guiyang, China, ⁶ Department of Cardiovascular Surgery, Union Hospital, Tongji Medical College, Huazhong University of Science and Technology, Wuhan, China

Objective: This study aimed to: (1) evaluate the association between myocardial fibrosis (MF) quantified by extracellular volume fraction (ECV) and myocardial strain measured by two-dimensional (2D)- and three-dimensional speckle-tracking echocardiography (3D-STE) and (2) further investigate which strain parameter measured by 2D- and 3D-STE is the more robust predictor of MF in heart transplant (HT) recipients.

Methods: A total of 40 patients with HT and 20 healthy controls were prospectively enrolled. Left ventricular (LV)-global longitudinal strain (GLS), global circumferential strain (GCS), and global radial strain (GRS) were measured by 2D- and 3D-STE. LV diffuse MF was defined by cardiovascular magnetic resonance (CMR)-ECV.

Results: The HT recipients had a significantly higher native T1 and ECV than healthy controls (1043.8 ± 34.0 vs. 999.7 ± 19.7 ms, $p < 0.001$; 26.6 ± 2.7 vs. $24.3 \pm 1.8\%$, $p = 0.02$). The 3D- and 2D-STE-LVGLS and LVGCS were lower ($p < 0.005$) in the HT recipients than in healthy controls. ECV showed a moderate correlation with 2D-LVGLS ($r = 0.53$, $p = 0.002$) and 3D-LVGLS ($r = 0.60$, $p < 0.001$), but it was not correlated with 2D or 3D-LVGCS, or LVGRS. Furthermore, 3D-LVGLS and 2D-LVGLS had a similar correlation with CMR-ECV ($r = 0.60$ vs. 0.53 , $p = 0.670$). A separate stepwise multivariate linear analysis showed that both the 2D-LVGLS ($\beta = 0.39$, $p = 0.019$) and 3D-LVGLS ($\beta = 0.54$, $p < 0.001$) were independently associated with CMR-ECV.

Conclusion: CMR marker of diffuse MF was present in asymptomatic patients with HT and appeared to be associated with decreased myocardial strain by echocardiography. Both the 2D- and 3D-LVGLS were independently correlated with diffuse LVMF, which may provide an alternative non-invasive tool for monitoring the development of adverse fibrotic remodeling during the follow-up of HT recipients.

Keywords: heart transplant, diffuse myocardial fibrosis, cardiovascular magnetic resonance, extracellular volume fraction, speckle tracking echocardiography

INTRODUCTION

Heart transplant (HT) is the most effective treatment for patients with end-stage heart failure (1). The outcome of HT has significantly improved owing largely to advances in immunosuppressive therapy and the management of long-term complications. However, myocardial fibrosis (MF) is a commonly demonstrated histopathologic feature and is associated with a higher risk of adverse cardiac events and death after HT (2–9). Therefore, a reliable non-invasive method for monitoring the development of fibrotic remodeling early may be desirable during the follow-up of patients with HT and can assist to risk stratification in HT recipients.

Histological biopsy is the gold standard for the assessment of MF, but it is invasive and not practical for serial follow-up after HT. Besides, the biopsied region only reflects the local pathological information and cannot quantify diffuse MF. However, numerous studies have validated that diffuse MF can be measured non-invasively by extracellular volume fraction (ECV) that was derived from cardiovascular magnetic resonance (CMR) in various cardiovascular diseases (10–13). Furthermore, previous studies have reported that two-dimensional speckle-tracking echocardiography (2D-STE)-derived myocardial strain may be a robust indicator to predict MF (14–16). However, 2D-STE is time-consuming and is affected by the through-plane motion during a cardiac cycle and the transplanted hearts would show noteworthy translational motion during the cardiac phase, which can aggravate the “out-of-plane phenomenon” of 2D-STE. Three-dimensional (3D)-STE can overcome the limitation of plane dependency existing in 2D-STE. Moreover, 3D-STE requires less time to acquire and analyze images (17). Nevertheless, the predictive value of myocardial strain for diffuse MF in HT recipients and whether 3D-STE is superior to 2D-STE remained unknown.

Therefore, this study aimed to: (1) evaluate the association between MF and myocardial strain measured by 2D- and 3D-STE and (2) further investigate which strain parameter measured by 2D- and 3D-STE is the more robust predictor of MF defined by CMR-ECV in HT recipients.

MATERIALS AND METHODS

Study Population

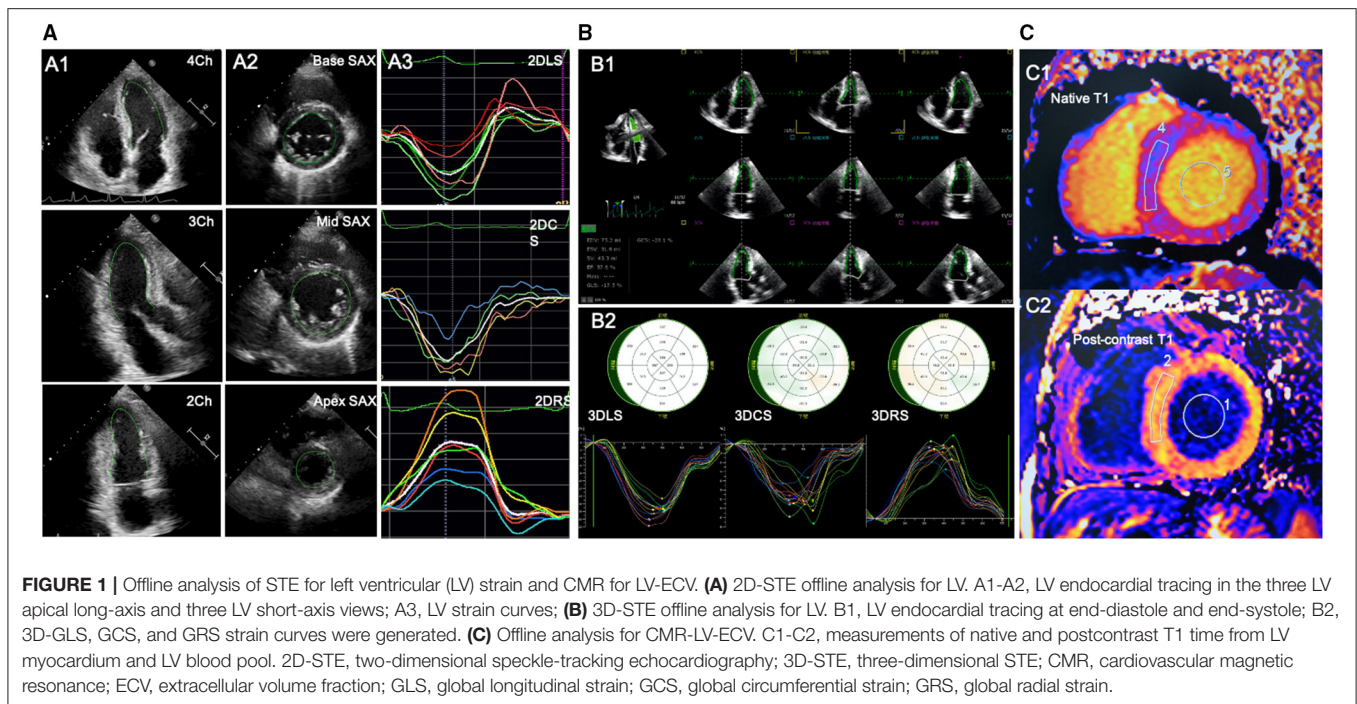
A total of 50 asymptomatic patients with HT who were scheduled for echocardiogram at their routine follow-up examinations

were prospectively enrolled in this study. As myocardial edema due to inflammation can expand the extracellular volume and increase native T1 times, patients with acute rejection (AR) at the time of recruitment were excluded. Patients with the following conditions were also excluded: time after HT < 6 months, left ventricular ejection fraction (LVEF) < 50%, significant coronary allograft vasculopathy (CAV), uncontrolled hypertension, uncontrolled blood glucose, renal failure, arrhythmia, and poor image quality. There were 10 patients excluded due to poor echocardiographic image quality ($n = 6$) and arrhythmia ($n = 4$). The remaining 40 patients were included in the final analysis. Demographic data including sex, age, height, and weight at the time of echocardiographic examination were obtained. Clinical data including recipient age, weight at HT, bypass time, ischemia time, donor age, weight, and history of AR and CAV were collected from a medical record review. Additionally, 20 healthy volunteers with a similar distribution of sex and age to the HT group were recruited as the control group. They had no history of hypertension, diabetes mellitus, renal failure, or other organic diseases based on physical examinations, biochemical tests, ECG, and echocardiography that were enrolled as a control group.

This study was approved by the Ethics Committee of Tongji Medical College, Huazhong University of Science and Technology, and all the participants provided a written informed consent.

Conventional 2D Echocardiography

All the 2D, Doppler, and 3D images were acquired by using a commercially available system (EPIQ 7C, Philips Medical Systems, Andover, Massachusetts, USA) with S5-1 and X5-1 transthoracic echocardiography transducers. Four heartbeat images were collected and stored in digital format. All the echocardiographic parameters were acquired according to the published guidelines (18). LV diameter was measured at end-diastole from the parasternal long-axis. Doppler mitral valve peak early (E) and late (A) diastolic velocities and E/A velocity ratio were measured on apical four-chamber view. The mean value of early diastolic mitral annular tissue velocity and left ventricular lateral wall tissue velocity (e') was measured by using tissue Doppler imaging. The LV Tei index was defined as the ratio of isovolumic time divided by ejection time with the use of tissue Doppler of the mitral annulus.



Left Ventricular Myocardial Strain Measured by 2D-STE and 3D-STE

The 2D myocardial strain was performed on the 2D cardiac performance analysis 1.2 software (TomTec Imaging Systems, Unterschleissheim, Germany, UK) in the 2D echocardiographic images with a frame rate of 50–70 MHz. LV longitudinal strain was determined by endocardial tracing in the apical four-, three-, and two-chamber views. LV circumferential and radial strain were measured by endocardial tracing in the basal, middle, and apical level of LV short-axis views on a frame-by-frame basis during one cardiac cycle. If the tracking was suboptimal, manual adjustment was performed. The LV global longitudinal strain (LVGLS), LV global circumferential strain (LVGCS), and LV global radial strain (LVGRS) were defined as the average peak strain values automatically generated from the 16 segmental strain curves by the software (**Figure 1A**).

The 3D-STE was performed on the four-dimensional (4D) LV-Analysis 3.1 Software (TomTec Imaging systems, Unterschleissheim, Germany, UK) in the 3D LV full-volume images with frame rate of 19–23 MHz. After selecting the center of the mitral annulus line and the apex of the left ventricle at end-diastole, the workstation would track the LV endocardium automatically and the manual adjustment was performed in case of unsatisfactory tracking. The same procedure was performed at the end-systolic frame. Subsequently, the software would perform the 3D-STE throughout the cardiac cycle. Ultimately, the 3D-LV-end-diastolic volume (EDV), end-systolic volume (ESV), LVEF, and the myocardial strain would be generated automatically. LVGLS, LVGCS, and LVGRS, respectively, were calculated as the average peak systolic longitudinal, circumferential, and radial strain of all the 16 LV segments (**Figure 1B**). Subjects with two or more inadequately tracked segments were removed from the analysis.

Cardiovascular Magnetic Resonance Images Acquired and Analyzed

Cardiovascular magnetic resonance imaging was performed with a 1.5-Tesla system (MAGNETOM Aera, Siemens Healthineers, Erlangen, Germany, UK). CMR examination was performed within 24 h of the echocardiography examination. Three long axes and a set of contiguous short-axis cine images of LV were acquired with a steady-state free precession sequence during breath-hold of 10–15 s. The cine image parameters were as follows: repetition time (TR)/echo time (TE), 38.09/1.21 ms; slice thickness, 8 mm; field of view, $340 \times 255 \text{ mm}^2$; matrix, 256 pixels \times 205 pixels; and flip angle, 80° . T1 mapping was performed on three standard LV short-axis slices before and 15 min after the administration of a bolus of gadopentetate dimeglumine contrast agent (0.2 mmol/kg, Magnevist, Bayer Healthcare, Berlin, Germany, UK) by using a modified Look-Locker inversion recovery (MOLLI) sequence with a 5- and 3-sampling scheme. The typical MOLLI sequence parameters were: TR/TE, 255.76/1.01 ms; slice thickness, 8 mm; matrix, 144 \times 256 pixels; flip angle, 35° ; and scan time, 11 s. The parameters of postcontrast T1 were similar to those of the native T1, except for a TE of 1.12 ms and a TR of 359.76 ms. Image acquisitions at LV basal, middle, and apical short-axis slices in diastole were performed before and 15 min after the injection of gadolinium, respectively.

Cardiovascular magnetic resonance data were analyzed with a commercial software (Argus, Siemens Healthineers, Erlangen, Germany, UK) by an experienced reader blinded to the echocardiographic results. Regions of interest were drawn in the blood and a midwall region of the myocardium and copied between the pre- and postcontrast T1 and ECV maps. To measure the T1 value of blood, a circular region of interest was positioned in the LV cavity, avoiding papillary muscle (**Figure 1C**). Then,

the ECV was calculated from the native and postcontrast T1 time, along with a hematocrit correction that was obtained on the same day of the CMR scanning according to the well-established formula (19).

Reproducibility

To evaluate the reproducibility of 2D-STE and 3D-STE measurements, a total of 20 subjects (including 10 HT recipients and 10 healthy controls) were selected randomly. For intraobserver variability, analysis of the first 2D-STE and 3D-STE data set of the 20 subjects (including 10 HT recipients and 10 healthy controls) was repeated 2–4 weeks later by the same primary investigator. For interobserver variability, the data set was analyzed by two blinded investigators.

Statistical Analysis

Continuous variables are presented as mean \pm SD or median [interquartile range (IQR)] and categorical variables are presented as absolute numbers (percentages). The unpaired two-sample *t*-test or the Mann–Whitney *U*-test was used to compare continuous variables and the chi-squared test or the Fisher's exact test was used to compare categorical variables between the HT and control group. Correlations between continuous variables were evaluated with the Pearson's correlation coefficients. Potential predictors (demographic, clinical, LV conventional function parameters, and myocardial strains) of ECV in HT recipients were identified by the univariate linear regression analysis. The variables with univariate $p < 0.10$ were included in the multivariate linear regression analysis. To avoid collinearity issues, the multivariate stepwise linear regression analysis for 2D-LVGLS and 3D-LVGLS (model 1 for 2D-LVGLS and model 2 for 3D-LVGLS) was performed separately, along with those echocardiographic and clinical variables that demonstrated a univariate $p < 0.10$. The interobserver and intraobserver variability of the 10 HT recipients and 10 healthy volunteers were assessed by the intraclass correlation coefficients (ICCs) and the Bland–Altman analyses. Comparison of correlation coefficients was performed with the MedCalc version 19.0.4 (MedCalc Software, Ostend, Belgium, UK). All the statistical analyses, except for the comparison of correlation coefficients, were performed with SPSS Statistics version 23.0 (IBM, Armonk, New York, USA). $p < 0.05$ was considered as statistically significant.

RESULTS

Clinical Characteristics

The baseline clinical characteristics of the 40 patients with HT are given in **Tables 1, 2**. The most prominent etiology for HT was dilated cardiomyopathy. The echocardiographic studies occurred at a median of 1.2 years after HT (IQR: 1.0–2.9 years). No patients had clinically significant AR or CAV when they were enrolled in this study. Immunosuppression regimens varied, but tacrolimus, mycophenolate mofetil, and prednisone were commonly used. Aspirin and statin were also frequently used.

TABLE 1 | Clinical characteristics of the 40 patients with HT.

Parameters	Value
Characteristics Pre-HT	
Recipient	
Men, <i>n</i> (%)	30 (75)
Age, (years)	43 \pm 13
Weight, (kg)	58 (50, 65)
Etiology for transplantation, <i>n</i> (%)	
Dilated cardiomyopathy	24 (60)
Ischemic cardiomyopathy	8 (20)
Valvular heart disease	3 (7.5)
Hypertrophic cardiomyopathy	1 (2.5)
Complex congenital heart disease	1 (2.5)
Other disease	3 (7.5)
Invasive mPAP, (mmHg)	38 \pm 14
Bypass time, (min)	97 (83, 115)
Aortic clamp time (min)	30 (27, 37)
Donor	
Age, (years)	35 \pm 10
Weight, (kg)	65 (55, 65)
Weight ratio, (donor/recipient)	1.1 \pm 0.3
Ischemic time, (min)	333 (195, 380)
Characteristics at echocardiographic examination	
Time since transplantation, (years)	1.2 (1.0, 2.9)
Surgical technique	
Biatial technique, <i>n</i> (%)	14 (35)
Bicaval technique, <i>n</i> (%)	26 (65)
History of AR, <i>n</i> (%)	4 (10)
Immunosuppressant medications	
Tacrolimus, <i>n</i> (%)	35 (87.5)
Sirolimus/everolimus, <i>n</i> (%)	6 (15.0)
Cyclosporine, <i>n</i> (%)	5 (12.5)
Mycophenolate mofetil, <i>n</i> (%)	37 (92.5)
Prednisone, <i>n</i> (%)	32 (80.0)
Aspirin, <i>n</i> (%)	26 (65.0)
Statin, <i>n</i> (%)	25 (62.5)
ACE inhibitor/ARB, <i>n</i> (%)	15 (37.5)
Calcium-channel blocker, <i>n</i> (%)	18 (45.0)
Beta-blocker, <i>n</i> (%)	18 (45.0)

AR, acute rejection; HT, heart transplant; mPAP, mean pulmonary arterial pressure.

Echocardiographic and CMR Findings

Comparisons of echocardiographic and CMR parameters in the 40 patients with HT and 20 healthy controls are shown in **Table 2**. Compared with healthy controls, patients with HT had a significantly greater E/A ratio of the mitral valve and shorter deceleration time (DT) of E wave, which may suggest impaired LV diastolic function. Concerning LV systolic function, patients with HT had lower 3D-LVEF than the healthy controls (62.4 \pm 5.5 vs. 66.1 \pm 3.9%, $p = 0.008$), but remained within the normal range. However, HT group showed impaired 2D-LVGLS, 2D-LVGCS, 3D-LVGLS, and 3D-LVGCS. In contrast, the two groups did not differ in 2D- and 3D-LVGRS. Moreover, a weak

TABLE 2 | Demographic information, echocardiographic, and CMR findings of the HT group and control group.

Parameters	Control group (n = 20)	HT group (n = 40)	P-value
Demographic information at echocardiography examination			
Men (%)	14 (70%)	34 (75%)	0.68
Age (years)	45 ± 11	45 ± 14	0.944
Height (cm)	168 ± 8	166 ± 8	0.482
Weight (kg)	65 ± 6	62 ± 13	0.071
BSA (m ²)	1.7 ± 0.1	1.7 ± 0.2	0.118
BMI (kg/m ²)	23 (21, 24)	22 (20, 24)	0.169
Obesity, n (%)	3 (15.0)	8(20.0)	0.637
HR (bpm)	67 ± 10	88 ± 7	<0.001
SBP (mmHg)	120 (110, 124)	120 (112, 126)	0.346
DBP (mmHg)	80 (70, 87)	80 (71, 85)	0.766
Echocardiographic findings			
LA, (mm)	33 ± 3	46 ± 7	<0.001
LVd, (mm)	44 ± 2	42 ± 4	0.093
IVST, (mm)	8.9 ± 0.8	9.6 ± 1.3	0.01
LVMl, (g)	72.0 ± 11.1	82.5 ± 17.6	0.007
Mitral valve			
E, (m/s)	0.7 ± 0.2	0.8 ± 0.2	0.366
A, (m/s)	0.6 ± 0.1	0.5 ± 0.1	<0.001
E/A ratio	1.2 ± 0.4	1.8 ± 0.4	<0.001
e', (cm/s)	11 ± 2	11 ± 2	0.528
E/e'	7 ± 2	8 ± 3	0.334
DT, (ms)	210 ± 45	182 ± 34	0.02
Tei index	0.36 ± 0.06	0.52 ± 0.11	<0.001
2D-LVGLS, (%)	-20.0 ± 2.5	-16.9 ± 2.3	<0.001
2D-LVGCS, (%)	-29.1 ± 3.3	-26.6 ± 4.7	0.038
2D-LVGRS, (%)	39.3 ± 6.0	37.8 ± 7.6	0.198
3D-LVEDV, (ml)	90.5 ± 17.8	72.0 ± 19.4	0.001
3D-LVESV, (ml)	30.7 ± 7.3	27.2 ± 9.3	0.013
3D-LVEF, (%)	66.1 ± 3.9	62.4 ± 5.5	0.008
3D-LVGLS, (%)	-20.8 ± 1.5	-17.2 ± 2.3	<0.001
3D-LVGCS, (%)	-31.5 ± 3.7	-28.3 ± 5.1	0.015
3D-LVGRS, (%)	42.3 ± 4.1	40.7 ± 6.3	0.339
CMR findings*			
Native T1 time, (ms)	999.7 ± 19.7	1043.8 ± 34.0	< 0.001
Post-contrast T1 time, (ms)	455.3 ± 24.5	429.8 ± 39.7	0.013
ECV, n (%)	24.3 ± 1.8	26.6 ± 2.7	0.002

2D, two dimensional; 3D, three dimensional; A, late diastolic inflow velocity; BSA, body surface area; CMR, cardiovascular magnetic resonance; DBP, diastolic blood pressure; DT, deceleration time of E; E, early diastolic inflow velocity; e', mean value of early diastolic mitral annular tissue velocity and left ventricular lateral wall tissue velocity; ECV, extracellular volume fraction; HR, heart rate; IVST, interventricular septum thickness; LA, left atrial diameter; LVd, left ventricular diastolic diameter; LVMl, left ventricular mass indexed to body surface area; LVEF, left ventricular ejection fraction; LVGLS, left ventricular global longitudinal strain; LVGCS, left ventricular global circumferential strain; LVGRS, left ventricular global radial strain; PA, pulmonary artery; SBP, systolic blood pressure.

*Means that 31 patients with HT and 20 healthy controls had the data of CMR findings.

to moderate but significant correlation of global strain values between the 2D- and 3D-STE was noted in the entire study population (LVGLS: $r = 0.57$, $p < 0.001$; LVGCS: $r = 0.46$, $p <$

0.001 ; LVGRS: $r = 0.45$, $p < 0.001$) (Figure 2). There were 31 of the 40 patients with HT and all the 20 healthy controls agreed to undergo CMR examination within 24 h of the echocardiography examination. Compared with healthy controls, the HT recipients showed significantly longer native T1 time (999.7 ± 19.7 vs. 1043.8 ± 34.0 ms, $p < 0.001$) and greater ECV (24.3 ± 1.8 vs. $26.6 \pm 6.7\%$, $p = 0.002$).

Relationships Between Diffuse LVMF and Clinical and Echocardiographic Parameters

The diffuse LVMF was defined by CMR-ECV in this study. The correlations between LV myocardial strain and CMR-ECV are shown in Figure 3. For 2D-LV myocardial strain, only 2D-LVGLS correlated with ECV ($r = 0.53$, $p = 0.002$), whereas LVGCS and LVGRS showed no correlation with ECV. Figure 3 also illustrates the association of 3D-LV myocardial strain with CMR-ECV. Similarly, as shown in Figures 3D-F, ECV only had correlation with 3D-LVGLS ($r = 0.60$, $p < 0.001$) and not had correlation with 3D-LVGCS or 3D-LVGRS. Moreover, 3D-LVEF did not correlate with CMR-ECV. Furthermore, there was no significant difference between the correlation of 2D-LVGLS with CMR-ECV and the correlation of 3D-LVGLS with CMR-ECV ($r = 0.53$ vs. $r = 0.60$, $p = 0.670$).

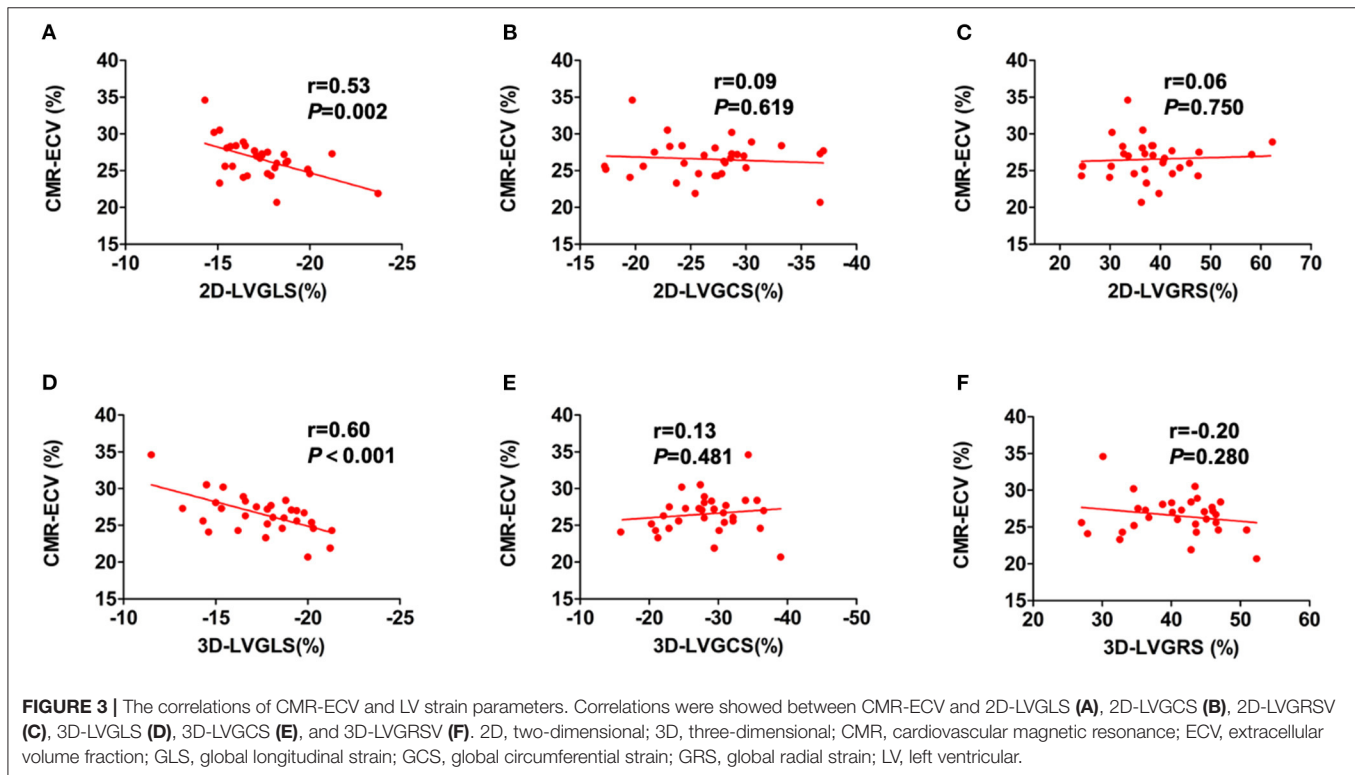
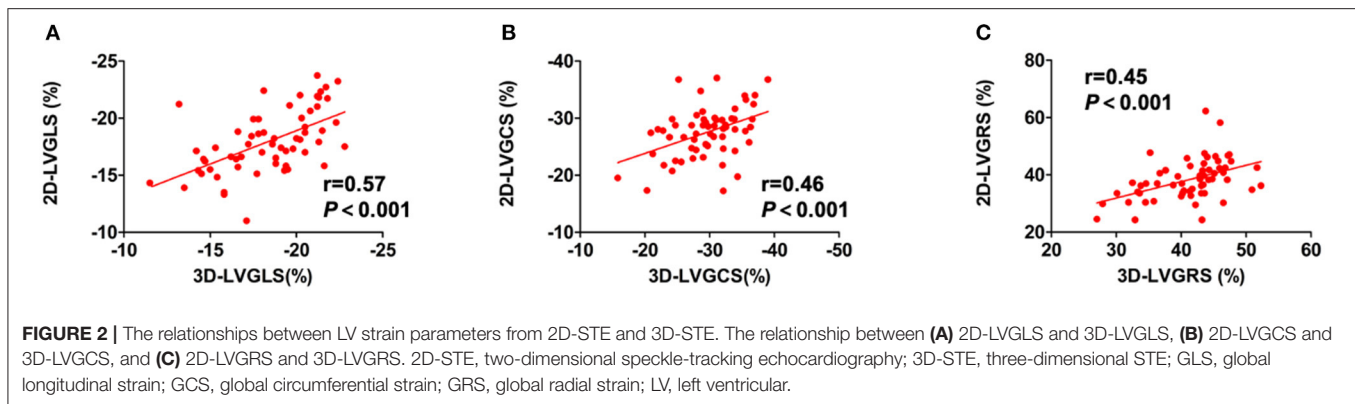
Table 3 shows the results of the univariate and multivariate linear regression analyses for the relationship between ECV and the clinical and echocardiographic variables in the HT recipients. The univariate regression analysis revealed that recipient age, time since HT, DT, 2D-LVGLS, and 3D-LVGLS were significantly correlated with ECV. In addition, 2D-LVGLS had correlation with 3D-LVGLS ($r = 0.57$, $p < 0.001$) (Figure 2). Therefore, to avoid the problems of collinearity, 2D-LVGLS and 3D-LVGLS were evaluated in two separate models. Finally, the stepwise multivariate regression analysis showed that 2D-LVGLS ($\beta = 0.39$, $p = 0.019$) and 3D-LVGLS ($\beta = 0.54$, $p < 0.001$) both were independently associated with CMR-ECV.

Reproducibility

The measurements obtained by 2D-STE and 3D-STE showed excellent reproducibility. The complete data of interobserver variability and intraobserver variability were shown in Table 4.

DISCUSSION

To the best of our knowledge, this is the first study to evaluate the level of diffuse LVMF with non-invasive CMR-ECV, further investigating the predictive value of 3D-STE-derived LV strain for diffuse LVMF in patients with post-HT, and directly compares its utility with that of 2D-STE-derived strains. The main findings of this study were: (1) the level of diffuse MF defined by CMR-ECV was higher even in asymptomatic patients with HT than in healthy controls; (2) the increased LVMF measured by CMR-ECV was correlated with 2D- and 3D-LVGLS, not correlated with LV-GCS, GRS, or ejection fraction (EF); and (3) both the 2D- and 3D-LVGLS were independently correlated with the extent of diffuse LVMF in HT recipients.



Left Ventricular MF in Patients With HT

The MF is a commonly demonstrated histopathologic feature in patients with HT and its correlation with a higher risk of adverse clinical outcome has been validated by the previous studies (2–5). Adverse fibrotic myocardial remodeling is a suspected long-term sequela of HT recipients. Therefore, it is clinically crucial to quantify the MF in the transplanted hearts at an early stage.

Histological biopsy is the gold standard for assessing MF, but it is invasive. The myocardial samples by the biopsy cannot accurately assess the diffuse MF. Furthermore, the endomyocardial biopsy is usually performed from the right ventricular side in the transplanted hearts and, thus, can not necessarily reflect LV information (1). Recently, the T1 time and ECV measured by CMR T1 mapping have emerged as a reliable non-invasive method for quantifying diffuse MF. However,

previous studies showed high variability in native T1 time for assessing MF (20, 21). However, compared to native T1 time, myocardial ECV, which was derived from myocardial and blood pre- and post-contrast T1 relaxation time changes, has been validated as a preferred non-invasive method for quantifying actual diffuse MF in various cardiovascular diseases (10–13). Therefore, we selected the non-invasive CMR-ECV to measure diffuse MF in the patients after HT. This study proved that ECV was higher even in asymptomatic patients with HT with normal LVEF than in healthy controls, indicating the increased diffuse MF in the transplanted hearts. The increased MF in the transplanted hearts was consistent with a previous study that measured the MF through the histological biopsy or CMR T1 mapping (3–7, 22). AR, CAV, ischemic injury of the donor's heart, and postoperatively immunosuppressive therapy all may lead to

TABLE 3 | Univariate and multivariate linear regression analysis for ECV in patients with HT ($n = 31$).

Variables	Univariate analysis		Multivariate analysis			
	β	P-value	Model 1 + 2D-LVGLS		Model 2 + 3D-LVGLS	
			β	P-value	β	P-value
Pre-HT						
Donor age, (years)	0.21	0.280				
Donor weight, (kg)	-0.08	0.663				
Recipient age, (years)	0.37	0.044	0.18	0.267	0.09	0.543
Recipient weight, (kg)	0.17	0.378				
Weight ratio, (donor/recipient)	-0.02	0.923				
Invasive mPAP, (mmHg)	0.21	0.276				
CPB time, (min)	0.10	0.592				
Aortic clamp time, (min)	0.11	0.559				
Ischemic time, (min)	-0.07	0.737				
Post-HT						
HR, (bpm)	-0.13	0.496				
SBP, (mmHg)	-0.24	0.192				
DBP, (mmHg)	-0.22	0.233				
History of ACR, (yes vs no)	-0.19	0.302				
Time since transplantation, (years)	0.42	0.018	0.24	0.139	0.32	0.022
Mitral valve						
E/A ratio	0.04	0.822				
E/e'	0.17	0.376				
DT, (ms)	-0.32	0.079	-0.23	0.134	-0.29	0.039
LV Tei index	0.16	0.398				
2D-LVGLS, (%)	0.53	0.002	0.39	0.019		
2D-LVGCS, (%)	0.09	0.619				
2D-LVGGRS, (%)	0.06	0.750				
3D-LVEF, (%)	0.26	0.151				
3D-LVGLS, (%)	0.60	<0.001			0.54	<0.001
3D-LVGCS, (%)	0.13	0.481				
3D-LVGGRS, (%)	-0.20	0.280				
3D-LVEF, (%)	-0.26	0.151				

Abbreviations as in **Tables 1, 2**.

MF of the transplanted hearts (2, 23, 24). Moreover, this study proved that CMR-ECV was positively correlated with time after HT, which corresponded to some other studies that indicated the MF may develop over time (3–5). Additionally, this study also proved that the ECV was correlated with the recipient age, which may suggest that recipient age would affect the allograft remodeling in the transplanted hearts. Furthermore, this study showed that the ECV did not correlate with ischemic time during transplantation, which was not in concordance with the study by Yuan et al. (22) but was in agreement with the study by Ide et al. (7). Therefore, the association between LVMF and the ischemic time needs to be further explored in the multicenter studies among broader research populations in the future.

Correlation Between LV Myocardial Strain and CMR-ECV

The echocardiographic myocardial strain can accurately quantify ventricular mechanical function and it has emerged

as a promising modality for predicting MF non-invasively and conveniently (14, 15). However, the correlation between the myocardial strain and MF in patients with post-HT has not been elucidated. Some studies have shown that increased LVMF measured by CMR-ECV was correlated with the decreased LV myocardial strain in a variety of heart diseases (16, 25–27). However, the studies about the association between 2D-myocardial strain and ECV show high variability and studies addressing which strain components might correlate best with ECV have not been seen. This is the first study to reveal the association between CMR-ECV and LV myocardial strain measured by 2D- and 3D-STE simultaneously in patients with HT.

This study showed that CMR-ECV both correlated with the 2D- and the 3D-LVGLS. A possible mechanism linking ECV to reduced systolic strain may be that the increased fibrosis leading to increased LV stiffness, which resulted in reduced

TABLE 4 | Intraobserver and interobserver reproducibility for the parameters of the two-dimensional and the three-dimensional speckle-tracking echocardiography.

	ICC (95% CI)	Bias	Limits of agreement
Intra-observer (n = 20)			
2D-LVGLS, (%)	0.95 (0.88-0.98)	0.1	-1.5~1.7
2D-LVGCS, (%)	0.94 (0.85-0.97)	0.2	-3.0~3.3
2D-LVGRS, (%)	0.87 (0.71-0.95)	1.0	-6.7~4.7
3D-LVGLS, (%)	0.97 (0.93-0.99)	0.1	-1.2~1.2
3D-LVGCS, (%)	0.92 (0.80-0.97)	0.3	-3.7~3.2
3D-LVGRS, (%)	0.90 (0.78-0.96)	0.8	-3.7~5.3
Inter-observer (n = 20)			
2D-LVGLS, (%)	0.93 (0.83-0.97)	0.1	-1.7~2.0
2D-LVGCS, (%)	0.90 (0.76-0.96)	1.2	-2.7~5.3
2D-LVGRS, (%)	0.85 (0.67-0.94)	1.3	-7.3~4.8
3D-LVGLS, (%)	0.95 (0.88-0.98)	0.1	-1.6~1.8
3D-LVGCS, (%)	0.87 (0.70-0.95)	0.3	-4.4~4.0
3D-LVGRS, (%)	0.86 (0.67-0.94)	0.8	-4.6~6.2

Abbreviations as in **Table 2**.

n = 20 means that there were 10 patients with HT and 10 healthy controls data used in this table.

end-diastolic muscle fiber length and, by the Frank–Starling law, reduced cardiac muscle contraction and systolic strain. The significant correlation between MF and GLS in the HT recipients in this study is in agreement with previous studies for other cardiovascular diseases (15, 16, 28). However, the increased ECV was not correlated with GCS or GRS in this study. This is possibly due to the fact that the LS mainly depends on the subendocardial layer and the subendocardial myocardium is sensitive to fibrosis (28). However, the CS mainly reflects the strain in the midmyocardium and RS is a change in the wall thickness of a length of the vertical line from a point on the endocardial border to a cross point on the epicardial border (29). In addition, patients with HT in our study had no severe complications at the time of CMR examination, such as AR and CAV in this study. Therefore, the extent of LV diffuse MF may be relatively mild in our subjects. Moreover, the early stage of MF mainly occurs in the endocardium and only LS can reveal this abnormality (29, 30). We believe that the aforementioned reasons may explain why only decreased GLS had a correlation with the increased ECV in the transplanted hearts.

Theoretically, compared with 2D-STE, 3D-STE is not affected by geometric modeling and out-of-plane motion, and it can evaluate the myocardial deformation in all the three spatial dimensions (17, 31). However, clinical testing and validation are needed to determine whether 3D-STE is superior to 2D-STE. The comparability of 2D- and 3D-STE has been studied extensively in healthy subjects and patients with various other cardiovascular diseases previously (17, 32, 33). However, the comparability of the association between 2D- and 3D-STE-derived strain and CMR evidence of diffuse MF has not been studied in patients post-HT simultaneously. This study made a direct comparison of strain values by 2D and 3D-STE in predicting the MF and

revealed that 2D-LVGLS and 3D-LVGLS provides comparable results. The image quality and spatial resolution of 3D-STE are suboptimal than 2D-STE. The lower frame rate of 3D-STE may not be sufficient to accurately capture all the phases of a cardiac cycle. In addition, patients with HT had a higher heart rate. The aforementioned limitations of 3D-STE may lead to the conclusion that it is not superior to 2D-STE in correlation with CMR-ECV.

Clinical Implications

This study proved that the level of diffuse MF defined by CMR-ECV was higher even in asymptomatic patients with HT than in healthy controls. Since MF is an adverse pathologic remodeling and can result in poor clinical outcomes, a reliable non-invasive method to monitor graft fibrosis would be clinically effective for the early identification of higher risk of patients with HT. This study showed that both 2D- and 3D-LVGLS were independently correlated with diffuse MF in HT recipients. Considering the correlation between 2D-STE or 3D-STE derived strain and MF is not robust and only presents up to 36% variations of MF. Therefore, CMR and cardiac biopsy cannot be replaced by these echocardiography modalities. Still this study suggested that measurements of 2D- and 3D-LVGLS may provide a valuable preliminary alternative non-invasive assessment of MF in the transplanted hearts, which may facilitate early risk stratification of HT recipients during follow-up examinations.

Study Limitations

This study is a single-center study and is limited by a relatively small sample size. The HT recipients with AR and CAV at the time of CMR were not included in this study. So, the range of diffuse MF in this study was relatively narrow. In addition, there were no results of the histological biopsy in this study. (Nevertheless, ECV has been validated as a valuable surrogate marker for the assessment for the diffuse MF). Moreover, 3D-STE is highly independent of image quality and its frame rate was lower. Last, as the strain parameters are vendor dependent and not interchangeable, our results may not apply to other software algorithms.

CONCLUSION

This study showed that CMR marker of diffuse MF was present in asymptomatic patients with HT and it was correlated with the 2D- and the 3D-LVGLS, not with LVGCS and LVGRS by echocardiography. The findings highlight the clinical superiority of the 2D- and the 3D-LVGLS over LVGCS, LVGRS, and other conventional parameters in predicting diffuse MF in HT recipients. 2D- and 3D-LVGLS may provide noninvasive tools for monitoring the development of adverse fibrotic remodeling during the serial follow-up of HT recipients.

DATA AVAILABILITY STATEMENT

The raw data supporting the conclusions of this article will be made available by the corresponding authors, without undue reservation.

ETHICS STATEMENT

This study was approved by the Ethics Committee of Tongji Medical College, Huazhong University of Science and Technology. The patients/participants provided their written informed consent to participate in this study.

AUTHOR CONTRIBUTIONS

WS, BL, LZ, and MX: conception and design of study. WS, XS, JW, SZ, YZ, CW, YX, and YY: acquisition of data. WS, XS, JW, ND, GW, YL, and QL: analysis and/or interpretation of data. JW, BL, LZ, and MX:

revised the manuscript. WS, XS, and JW: drafting the manuscript. QL, BL, LZ, and MX: revising the manuscript critically for important intellectual content. All authors contributed to the article and approved the submitted version.

FUNDING

This study was supported by the National Natural Science Foundation of China (Grant Numbers: 81922033, 81671705, 81727805, and 81530056) and the Key Research and Development Program of Hubei (Grant Number: 2020DCD015).

REFERENCES

- Badano LP, Miglioranza MH, Edvardsen T, Colafranceschi AS, Muraru D, Bacal F, et al. European Association of Cardiovascular Imaging/Cardiovascular Imaging Department of the Brazilian Society of Cardiology recommendations for the use of cardiac imaging to assess and follow patients after heart transplantation. *Eur Heart J Cardiovasc Imaging*. (2015) 16:919–48. doi: 10.1093/ehjci/jev139
- Sade LE, Hazirolan T, Kozan H, Ozdemir H, Hayran M, Eroglu S, et al. T1 mapping by cardiac magnetic resonance and multidimensional speckle-tracking strain by echocardiography for the detection of acute cellular rejection in cardiac allograft recipients. *JACC Cardiovasc Imaging*. (2019) 12:1601–14. doi: 10.1016/j.jcmg.2018.02.022
- Gramley F, Lorenzen J, Pezzella F, Kettering K, Himmrich E, Plumhans C, et al. Hypoxia and myocardial remodeling in human cardiac allografts: a time-course study. *J Heart Lung Transplant*. (2009) 28:1119–26. doi: 10.1016/j.healun.2009.05.038
- Armstrong AT, Binkley PF, Baker PB, Myerowitz PD, Leier CV. Quantitative investigation of cardiomyocyte hypertrophy and myocardial fibrosis over 6 years after cardiac transplantation. *J Am Coll Cardiol*. (1998) 32:704–10. doi: 10.1016/S0735-1097(98)00296-4
- Goland S, Siegel RJ, Burton K, De Robertis MA, Rafique A, Schwarz E, et al. Changes in left and right ventricular function of donor hearts during the first year after heart transplantation. *Heart*. (2011) 97:1681–6. doi: 10.1136/hrt.2010.220871
- Riesenkampff E, Chen CK, Kantor PF, Greenway S, Chaturvedi RR, Yoo SJ, et al. Diffuse myocardial fibrosis in children after heart transplantations: a magnetic resonance T1 mapping study. *Transplantation*. (2015) 99:2656–62. doi: 10.1097/TP.0000000000000769
- Ide S, Riesenkampff E, Chiasson DA, Dipchand AI, Kantor PF, Chaturvedi RR, et al. Histological validation of cardiovascular magnetic resonance T1 mapping markers of myocardial fibrosis in paediatric heart transplant recipients. *J Cardiovasc MagnReson*. (2017) 19:10. doi: 10.1186/s12968-017-0326-x
- Hughes A, Okasha O, Farzaneh-Far A, Kazmirczak F, Nijjar PS, Velangi P, et al. Myocardial fibrosis and prognosis in heart transplant recipients. *Circ Cardiovasc Imaging*. (2019) 12:e009060. doi: 10.1161/CIRCIMAGING.119.009060
- Pedrotti P, Vittori C, Facchetti R, Pedretti S, Dellegrottaglie S, Milazzo A, et al. Prognostic impact of late gadolinium enhancement in the risk stratification of heart transplant patients. *Eur Heart J Cardiovasc Imaging*. (2017) 18:130–7. doi: 10.1093/ehjci/jev186
- aus dem Siepen F, Buss SJ, Messroghli D, Andre F, Lossnitzer D, Seitz S, et al. T1 mapping in dilated cardiomyopathy with cardiac magnetic resonance: quantification of diffuse myocardial fibrosis and comparison with endomyocardial biopsy. *Eur Heart J Cardiovasc Imaging*. (2015) 16:210–6. doi: 10.1093/ehjci/jev183
- Nakamori S, Dohi K, Ishida M, Goto Y, Imanaka-Yoshida K, Omori T, et al. Native T1 mapping and extracellular volume mapping for the assessment of diffuse myocardial fibrosis in dilated cardiomyopathy. *JACC Cardiovasc Imaging*. (2018) 11:48–59. doi: 10.1016/j.jcmg.2017.04.006
- Fontana M, White SK, Banypersad SM, Sado DM, Maestrini V, Flett AS, et al. Comparison of T1 mapping techniques for ECV quantification. Histological validation and reproducibility of ShMOLLI versus multibreath-hold T1 quantification equilibrium contrast CMR. *J Cardiovasc MagnReson*. (2012) 14:88. doi: 10.1186/1532-429X-14-88
- Cui Y, Cao Y, Song J, Dong N, Kong X, Wang J, et al. Association between myocardial extracellular volume and strain analysis through cardiovascular magnetic resonance with histological myocardial fibrosis in patients awaiting heart transplantation. *J Cardiovasc Magn Reson*. (2018) 20:25. doi: 10.1186/s12968-018-0445-z
- Lisi M, Cameli M, Righini FM, Malandrino A, Tacchini D, Focardi M, et al. RV longitudinal deformation correlates with myocardial fibrosis in patients with end-stage heart failure. *JACC Cardiovasc Imaging*. (2015) 8:514–22. doi: 10.1016/j.jcmg.2014.12.026
- Cameli M, Mondillo S, Righini FM, Lisi M, Dokollari A, Lindqvist P, et al. Left ventricular deformation and myocardial fibrosis in patients with advanced heart failure requiring transplantation. *J Card Fail*. (2016) 22:901–7. doi: 10.1016/j.cardfail.2016.02.012
- Cameli M, Mondillo S, Righini FM, Lisi M, Dokollari A, Lindqvist P, et al. Diffuse interstitial fibrosis and myocardial dysfunction in early chronic kidney disease. *Am J Cardiol*. (2015) 115:1311–7. doi: 10.1016/j.amjcard.2015.02.015
- Saito K, Okura H, Watanabe N, Hayashida A, Obase K, Imai K, et al. Comprehensive evaluation of left ventricular strain using speckle tracking echocardiography in normal adults: comparison of three-dimensional and two-dimensional approaches. *J Am Soc Echocardiogr*. (2009) 22:1025–30. doi: 10.1016/j.echo.2009.05.021
- Lang RM, Badano LP, Mor-Avi V, Afilalo J, Armstrong A, Ernande L, et al. Recommendations for cardiac chamber quantification by echocardiography in adults: an update from the American Society of Echocardiography and the European Association of Cardiovascular Imaging. *J Am Soc Echocardiogr*. (2015) 28:1–39.e14. doi: 10.1016/j.echo.2014.10.003
- Flett AS, Hayward MP, Ashworth MT, Hansen MS, Taylor AM, Elliott PM, et al. Equilibrium contrast cardiovascular magnetic resonance for the measurement of diffuse myocardial fibrosis: preliminary validation in humans. *Circulation*. (2010) 122:138–44. doi: 10.1161/CIRCULATIONAHA.109.930636
- Bull S, White SK, Piechnik SK, Flett AS, Ferreira VM, Loudon M, et al. Human non-contrast T1 values and correlation with histology in diffuse fibrosis. *Heart*. (2013) 99:932–7. doi: 10.1136/heartjnl-2012-303052
- de Meester de Ravenstein C, Bouzin C, Lazam S, Boulij J, Amzulescu M, Melchior J, et al. Histological validation of measurement of diffuse interstitial myocardial fibrosis by myocardial extravascular volume fraction from Modified Look-Locker imaging (MOLLI) T1 mapping at 3 T. *J Cardiovasc Magn Reson*. (2015) 17:48. doi: 10.1186/s12968-015-0150-0
- Yuan Y, Cai J, Cui Y, Wang J, Alwalid O, Shen X, et al. CMR-derived extracellular volume fraction (ECV) in asymptomatic heart transplant recipients: correlations with clinical features and myocardial edema.

- Int J Cardiovasc Imaging.* (2018) 34:1959–67. doi: 10.1007/s10554-018-1421-2
23. Pickering JG, Boughner DR. Fibrosis in the transplanted heart and its relation to donor ischemic time. Assessment with polarized light microscopy and digital image analysis. *Circulation.* (1990) 81:949–58. doi: 10.1161/01.CIR.81.3.949
 24. Yamani MH, Haji SA, Starling RC, Tuzcu EM, Ratliff NB, Cook DJ, et al. Myocardial ischemic-fibrotic injury after human heart transplantation is associated with increased progression of vasculopathy, decreased cellular rejection and poor long-term outcome. *J Am Coll Cardiol.* (2002) 39:970–7. doi: 10.1016/S0735-1097(02)01714-X
 25. Zeng M, Qiao Y, Wen Z, Liu J, Xiao E, Tan C, et al. The association between diffuse myocardial fibrosis on cardiac magnetic resonance T1 mapping and myocardial dysfunction in diabetic rabbits. *Sci Rep.* (2017) 7:44937. doi: 10.1038/srep44937
 26. Kuruvilla S, Janardhanan R, Antkowiak P, Keeley EC, Adenaw N, Brooks J, et al. Increased extracellular volume and altered mechanics are associated with LVH in hypertensive heart disease, not hypertension alone. *JACC Cardiovasc Imaging.* (2015) 8:172–80. doi: 10.1016/j.jcmg.2014.09.020
 27. Park SJ, Cho SW, Kim SM, Ahn J, Carriere K, Jeong DS, et al. Assessment of myocardial fibrosis using multimodality imaging in severe aortic stenosis: comparison with histologic fibrosis. *JACC Cardiovasc Imaging.* (2019) 12:109–19. doi: 10.1016/j.jcmg.2018.05.028
 28. Wang J, Zhang Y, Zhang L, Tian F, Wang B, Xie Y, et al. Assessment of myocardial fibrosis using two-dimensional and three-dimensional speckle tracking echocardiography in dilated cardiomyopathy with advanced heart failure. *J Card Fail.* (2021) 27:651–61. doi: 10.1016/j.cardfail.2021.01.003
 29. Seo Y, Ishizu T, Atsumi A, Kawamura R, Aonuma K. Three-dimensional speckle tracking echocardiography. *Circ J.* (2014) 78:1290–301. doi: 10.1253/circj.CJ-14-0360
 30. de Leeuw N, Ruiter DJ, Balk AH, de Jonge N, Melchers WJ, Galama JM. Histopathologic findings in explanted heart tissue from patients with end-stage idiopathic dilated cardiomyopathy. *Transpl Int.* (2001) 14:299–306. doi: 10.1007/s001470100339
 31. Yodwut C, Weinert L, Klas B, Lang RM, Mor-Avi V. Effects of frame rate on three-dimensional speckle-tracking-based measurements of myocardial deformation. *J Am Soc Echocardiogr.* (2012) 25:978–85. doi: 10.1016/j.echo.2012.06.001
 32. Nagata Y, Takeuchi M, Wu VC, Izumo M, Suzuki K, Sato K, et al. Prognostic value of LV deformation parameters using 2D and 3D speckle-tracking echocardiography in asymptomatic patients with severe aortic stenosis and preserved LV ejection fraction. *JACC Cardiovasc Imaging.* (2015) 8:235–45. doi: 10.1016/j.jcmg.2014.12.009
 33. Trache T, Stöbe S, Tarr A, Pfeiffer D, Hagendorf A. The agreement between 3D, standard 2D and triplane 2D speckle tracking: effects of image quality and 3D volume rate. *Echo Res Pract.* (2014) 1:71–83. doi: 10.1530/ERP-14-0025
- Conflict of Interest:** The authors declare that the research was conducted in the absence of any commercial or financial relationships that could be construed as a potential conflict of interest.
- Publisher's Note:** All claims expressed in this article are solely those of the authors and do not necessarily represent those of their affiliated organizations, or those of the publisher, the editors and the reviewers. Any product that may be evaluated in this article, or claim that may be made by its manufacturer, is not guaranteed or endorsed by the publisher.
- Copyright © 2021 Sun, Shen, Wang, Zhu, Zhang, Wu, Xie, Yang, Dong, Wang, Li, Lv, Liang, Zhang and Xie. This is an open-access article distributed under the terms of the Creative Commons Attribution License (CC BY). The use, distribution or reproduction in other forums is permitted, provided the original author(s) and the copyright owner(s) are credited and that the original publication in this journal is cited, in accordance with accepted academic practice. No use, distribution or reproduction is permitted which does not comply with these terms.